ECOLOGY

Hydrochemical basis of marine waters biological productivity surrounding Svalbard archipelago

Alexey Namyatov[1], Pavel Makarevich[1], Igor Tokarev[2], and Ivan Pastuhov[1]

[1]Murmansk Marine Biological Institute, Russian Academy of Sciences, ul. Vladimirskaya, 17, Murmansk, 183010, Russian Federation
[2]Centre for X-ray Diffraction Studies, Research Park of Saint Petersburg State University, per. Dekabristov, 16, Saint Petersburg, 199155, Russian Federation

Address correspondence and requests for materials to Alexey Namyatov, alexey.nmyatov@yandex.ru

Abstract

This study provides a rather new approach to research on a portion of general biological production of marine ecosystems, namely on primary production. The methodology presented consists of two blocks of techniques. The hydrological block provides for an estimate of the amounts of basic water masses, the estimate being based on the salinity and $\delta^{18}O$ stable isotope value. The techniques of the ecosystem block provide for a calculation of primary production based on the water mass composition, nutrients concentrations in the cores of the water masses, and changes in nutrients reserves. The rate of the nutrients reserve change is corrected by the non-productive component caused by the inflow or outflow of the nutrient as a result of advection or exchange with underlying layers. Another correction is related to nutrient regeneration going in parallel to photosynthesis. The technique was tested and verified in the waters around the Svalbard archipelago. By using a combination of $\delta^{18}O$ isotope parameter (with an intention to add $\delta^{2}H$ in the future), salinity, and nutrients composition, the present methodology allows to consider the domain of the marine ecosystem comprising its hydrological, hydrochemical, and hydrobiological (phytoplankton) processes as a single system of their relationships.

Keywords: Barents Sea, nutrients, phytoplankton, primary production, new production, photosynthesis

Introduction

Due to its geographical position and the peculiarities of its land and marine ecosystems development, the Svalbard archipelago provides for a unique ground to examine the whole range of responses of high Arctic natural environments to external impact, both natural and human-induced. Among the purposes of such research is revealing and examining the regions that potentially provide the best opportunities as a feeding resource for fish and other farming facilities, that is, regions with the highest nutrients supply to phytoplankton. Phytoplankton plays a crucial role in the development of feeding resources for various hydrobionts, including commercial fish (Arzhanova and Zubarevich, 1997). The Barents Sea waters, including those around the Svalbard archipelago, form a highly productive area, accounting for 49 % of the whole primary production of the panarctic shelf (Sakshaug, 2004, quoted after Reigstad et al., 2011). Currently, there are several approaches to assessing phytoplankton production.

One group of such techniques is based on direct measurements of summer primary production by two traditional methods, namely the oxygen and radiocarbon methods. One of the recent studies *"compared three common methods for estimating PP in the European Arctic Ocean: (1) production of 18O-labeled oxygen (GPP-18O), (2) changes in dissolved oxygen (GPP-DO), and (3) incorporation*

Citation: Namyatov, A., Makarevich, P., Tokarev, I., and Pastuhov, I. 2023. Hydrochemical basis of marine waters biological productivity surrounding Svalbard archipelago. Bio. Comm. 68(1): 30–48. https://doi.org/10.21638/spbu03.2023.104

Authors' information: Alexey Namyatov, PhD, Leading Researcher, orcid.org/0000-0002-9276-3632; Pavel Makarevich, PhD, Chief Researcher, orcid.org/0000-0002-7581-862X; Igor Tokarev, PhD, Leading Researcher, orcid.org/0000-0003-1095-0731; Ivan Pastuhov, Junior Researcher, orcid.org/0000-0003-2090-0287

Manuscript Editor: Evgeny Abakumov, Department of Applied Ecology, Faculty of Biology, Saint Petersburg State University, Saint Petersburg, Russia

Received: July 13, 2022;

Revised: December 12, 2022;

Accepted: February 1, 2023.

Funding: The study was performed as a part of the state task of the Ministry of Science and Higher Education state research project of the Murmansk Marine Biological Institute of the Russian Academy of Sciences.

Ethics statement: This paper does not contain any studies involving human participants or animals performed by any of the authors.

Competing interests: The authors have declared that no competing interests exist.

rates of 14C-labeled carbon into particulate organic carbon (14C-POC) and into total organic carbon (14C-TOC, the sum of dissolved and particulate organic carbon) The choice of either method should be guided by the specific question being addressed. In this way, the methods are complementary. For example, the combination of 14C-TOC and 14C-POC provides information of food supply (as DOC) for the microbial food web, not available from the oxygen methods. Furthermore, 14C-POC represents the phytoplankton carbon production needed when quantifying the food available for higher trophic levels. The DO methods provide independent estimates of community respiration (CR) and net community production (NCP)" (Sanz-Martín et al., 2019).

Another approach is related to assessing primary production using chlorophyll values, both measured directly in sea water samples and defined based on data from remote Earth sensing (Vernet et al., 2021).

The third approach is model calculation, comprising both hydrodynamic and ecosystem models (Reigstad et al., 2011; Slagstad, Wassmann, and Ellingsen, 2015). In one of the recent studies, *"NPP (net primary production) is estimated by two independent approaches already established as best for estimating Arctic productivity: a physically-biologically coupled, regional 3D ocean model (SINMOD) and a spectrally-resolved, light-photosynthesis model of primary production (UQUAR-Takuvik model) that is applied to satellite observations of phytoplankton chlorophyll a, which is derived from ocean color remote sensing (OCRS)"* (Vernet et al., 2021).

The fourth approach is using solid matter particles traps with further removal of inorganic carbon (Tamelander et al., 2013). Tamelander's 2013 study demonstrates a change of stoichiometric ratio in the Arctic Ocean. For the Barents Sea, the POC:PON (particulate organic carbon (POC) to nitrogen (PON)) atomic ratio was 8.5 ± 1.8, while the Redfield-Richards ratio, considered to be fundamental and typically applied in many primary production estimates, is 6.62 (Redfield, 1934; 1958; Richards, 1958). Not only has an examination of POC, chlorophyll a, and phytoplankton to the north of the Svalbard archipelago shown that the zone around the ice edge is the most productive area in this region, but also intense blooming and high rates of POC and PON export were registered in the ice-covered waters (Dybwad et al., 2021).

The fifth approach is based on estimating nutrients consumption and calculating primary production using average stoichiometric ratios. A great advantage of this approach is the relative simplicity of the chemical analysis required to define nutrients concentrations and a large database of these values that has been accumulated over the years. Primary production calculation technique is based on studies implemented in the previous century. In their works, A. P. Vinogradov (1939), R. Fleming (Sverdrup, Johnson, and Fleming, 1942), and L. Cooper (Cooper, 1937; 1938) provided phosphorus and nitrogen concentrations in phytoplankton and in the water. A group of authors (V. N. Ivanenkov, V. V. Sapozhnikov, V. A. Konnov, Yu. F. Lukashev, I. V. Sokolova, B. V. Volostykh, A. N. Gusarova) summarised these studies in their monograph "Chemistry of the Ocean" (Bordovsky and Ivanenkov, 1979). In a later study (Sapozhnikov and Metrevely, 2015), V. V. Sapozhnikov and M. P. Metreveli described thoroughly the history of organic matter stoichiometric modelling. As they demonstrate in their work, *"the stoichiometric model has allowed hydrochemistry to become a field of quantitative research, providing a possibility to calculate primary production based on the amounts of phosphates, nitrates, or silicon used up by phytoplankton, or to estimate nutrients regeneration rate using available data on the oxygen consumed, etc."*

Usually, several types of primary production are distinguished. General, or gross primary production, GPP, is the amount of chemical energy, typically expressed in terms of carbon biomass, that autotrophic communities create in a given period of time. Part of this energy is used in the autotrophs breathing. The remaining fixed energy (that is, the mass of the photosynthate) is called net primary production (NPP).

On the other hand, during the growing season, the amount of nutrients in the euphotic layer is replenished by their regeneration. Dugdale and Goering (Dugdale and Goering, 1967) introduced the concept of "new" and "regenerated" primary production; their study was based on incubations using ^{15}N-labelled nitrate and ammonium. Within this framework, general primary production (GPP) = new PP + regenerated PP.

Gross primary production (GPP) is defined as photosynthesis regardless of simultaneous algae respiration and of metabolism going on in heterotrophs. Net primary production (NPP) is GPP minus algae respiration. Net community production (NCP) is defined as GPP minus algae and heterotrophs respiration (Codispoti et al., 2013).

To calculate primary production based on carbon mass as a result of nutrients consumption, stoichiometric ratios are used, usually the Redfield-Richards ratio; Redfield-Richards molar ratio is C : Si : N : P = 106 : 23 : 16 : 1 (Redfield, 1958; Richards, 1958).

N. V. Arzhanova et al. showed in their studies (1995, 1997) that *"silicon regeneration is extremely slow as compared to that of nitrogen and phosphorus. Consequently, the least production values are, as a rule, equal to the decrease of nitrogen and phosphorus in the euphotic layer, while the largest ones to that of silicon. Moreover, an estimate of phytoplankton production by silicon concentration change allows to take into account the portion of production that was synthesised as part of nitrogen and phosphorus recycling"*. Nitrates support primary produc-

tion (new production); they are considered to represent the consumption of nutrients that were present in the beginning of the vegetation period or were brought to the euphotic zone from elsewhere.

To summarise the approach provided by Arzhanova et al. (1995) and analysed above, primary production calculated based on silicon (NCP_{Si}) corresponds to total production, while calculations based on nitrogen (NCP_N) provide for the "new" production value. In the present study, the same definitions and designations are used.

Today's techniques of biological productivity evaluation that are based on nutrients concentration changes rely on finding the difference between the amount of the nutrient observed and its amount that "was present in the given volume of water at the moment when its physical and chemical properties were forming in the near-surface ocean layer".

Several studies use the term "preformed" to designate such values (preformed phosphates ($P_п$), preformed nitrates ($N_п$), and preformed silicates ($Si_п$)). The calculation of preformed concentrations is based on stoichiometric ratios of phosphorus, nitrogen, and silicon to oxygen and carbon (Arzhanova and Zubarevich, 1995a; 1997; Kivva, 2014). Preformed concentrations are nutrient concentration baselines (maximum concentrations) against which concentration decrease during photosynthesis is assessed. This technique was used to estimate biological productivity of various water bodies that belong to the World Ocean, from the Bering Sea (Arzhanova and Zubarevich, 1995b; 1997; Kivva, 2014), the Sea of Okhotsk (Arzhanova and Zubarevich, 1997), the Barents Sea (Nesvetova, 2003; Titov, 2003) and to the waters surrounding the Antarctic (Batrak, 2009). To implement the technique, one needs to know winter nutrients concentrations that may be observed before the phytoplankton spring bloom. In the studies on the Bering Sea, these concentrations were defined as concentrations at the lower limit of the cold intermediate layer. The layer location ranged between 40 and 170 m. In the studies dedicated to the waters surrounding the Antarctic, this concentration was defined as the weighted average in the autumn and winter convection mixing layer. Such approaches may not always be applicable for several reasons:

— besides photosynthesis, vertical nutrients concentration change may be due to the surface layer containing a different water mass with a different initial composition of nutrients; this is characteristic of the south-eastern part of the Barents Sea and of the Kara and Laptev Seas;
— besides photosynthesis, oxygen concentration change may be related to an exchange with other water layers and with the atmosphere;
— today, to evaluate a nutrient primary production, that is carbon consumption, based on that nutrient consumption, Redfield — Richard average stoichiometric ratios are used. But applying these ratios to phytoplankton with various species compositions can lead to major errors because of a significant variation of these ratios among different plankton groups. For example, the C : P ratio change in the phytoplankton differs by 37 % between diatom and peridinium plankton, C : N ratio change by 24 %, and C : Si ratio change — by 15 times (Bordovsky and Ivanenkov, 1979);
— in addition to the "productive" component, the "non-productive" component participates in nutrient concentration changes; it may vary due to a supply of the nutrient examined from the near-bottom layer, as well as to other processes.

All the limitations above concern the evaluation of a fundamental parameter, the baseline, that is the nutrient concentration before spring bloom. The present study provides for an alternative technique of marine ecosystems biological productivity (phytoplankton production) evaluation; this technique allows to avoid the limitations above to some extent and is independent both of the depth of the lower photosynthetic layer and of average stoichiometric ratios.

The fundamental statement, or hypothesis, underlying the proposed approach is that the nutrients stoichiometric ratios in the primary dominant phytoplankton groups do vary, and this variation is a significant one. The study aims to use this variation to evaluate the phytoplankton primary production.

The aims of the study are as follows:

— To present a technique and to demonstrate the results of applying the conservativeness of the $\delta^{18}O$ isotopic parameter to the evaluation of nutrient baseline concentrations before the spring bloom, which allows to define individual stoichiometric ratios of a particular sample.
— To compare the results achieved with the results of other studies.

Designations used in the text:

GPP — gross primary production;
NCP_{Si} — silicon-based net community production;
NCP_N — nitrogen-based net community production;
PP — primary production;
NPP — net primary production;
TOC — total organic carbon;
POC — particulate organic carbon;
PON — particulate organic nitrogen;
DO — dissolved oxygen

Materials and methods

The methodology presented consists of two blocks of techniques. The hydrological block provides for an estimate of the amounts of basic water masses, the estimate being based

on the salinity and stable isotope value, namely, in this case, $\delta^{18}O$. The techniques of the ecosystem block provide for a calculation of primary production based on water mass composition and changes in nutrients concentrations.

Primary Production (PP). Calculation Framework (Ecosystem Block)

First of all, in order to estimate the primary production by nutrients consumption, it is necessary to measure the consumption of the element's mineral phase in the course of photosynthesis. It might appear possible to do this using the difference between early spring and summer values. But this is appropriate only if the non-production part of the element reserve is insignificant. If there is a significant non-production portion of concentration change (such change being due to vertical exchange or to advection), it is necessary to take these components into account when estimating the photosynthesis-associated concentration changes. E. g., at the end of winter, before the onset of the photosynthesis, silicon concentration at the point under consideration was 300 μg/l. In the summertime, with increased river runoffs, silicon concentrations could reach 600 μg/l, if not for photosynthesis. Assume that as a result of elements consumption by photosynthesis, the concentration has decreased by 200–300 μg/l. That means, not only would merely considering the difference between winter and summer values conceal the decrease of the value in summer as compared to that in the winter, but in some cases even an increase thereof would be possible. Even if a decrease in the element concentration is revealed in these circumstances, ignoring the advection will cause an underestimation of the primary production. Ignoring vertical flows of nutrients could cause a similar effect.

As it is the first time that this technique is described, we explain it here in the most detail.

An example of a nutrient balance at a point is shown in Fig. 1.

Nutrient concentration measured at a point will constitute a combination of conservative and non-conservative concentrations (1).

$$C_{meas} = C_{con} \pm \Delta C_{non-con} \quad (1)$$

C_{meas}: is the resulting (measured) concentration.

C_{con}: is the conservative concentration that depends only on the mixing of different waters and neither on photosynthetic nor on geochemical activity (sedimentary sedimentation).

$\Delta C_{non\text{-}con}$: is the non-conservative component, consisting of the "productive" component C_{phyto} and the "non-productive" component C_{sed}.

C_{phyto}: is the concentration change resulting from the photosynthesis process or mineralization of organic matter — the "productive" component.

C_{sed}: is the concentration change resulting from an exchange with the underlying layers (precipitation of the substance in question or its entry from a lower layer) as a result of vertical mixing — "non-productive" component. C_{sed} also includes the inflow resulting from advection.

$$\Delta C_{non-con} = C_{phyto} + C_{sed} \quad (2)$$

In order to calculate the primary production based on the consumption of an element, it is necessary to determine the change in that element's concentration at a point resulting from photosynthesis. To do this, it is necessary to determine all the nutrient balance components.

Calculation of the conservative component

The conservative concentration can be determined using the following equation:

$$C_{con} = f_a \times C_a + f_r \times C_r + f_i \times C_i, \quad (3)$$

$$f_a + f_r + f_i = 1 \quad (4)$$

where: C_a = average concentration of the element in question in "pure" Atlantic water; *fa* = volume of the "pure" Atlantic water in the resulting water mass (%); C_r = average concentration of the element in "pure" river water; f_r = volume of "pure" river water in (%); C_i = average concentration of the element in the "ice water"; *i* = an index indicating that ice is concerned; *fi* = volume of the sea ice formed corrected by water density, or the volume of meltwater in %; for simplicity, we will call this parameter "ice water".

Concentrations of the nutrient *j* (*Caj, Crj, Cij*) in the initial water masses are shown in Table 1.

Table 1. Values of the parameters examined (*Caj, Crj, Cij*) in the initial water masses (μg/l)

Water mass	P-PO_4	N-NO_3	Si-SiO_3
Atlantic	23.4	114.2	135.3
River	26.2	80.6	3061
Ice	11.1	24.8	30.9

Atlantic water: For this water mass, average values of the parameters in question in the Atlantic waters entering the Barents Sea were taken, as determined for the layer of 0–200 m, in February, in the area within 71.5–73.5° N and 20–25° E. Values were selected from the general NODC database (Boyer et, al., 2018; 2019). The period of the year and the sample layer were chosen as to ensure maximum values of the elements' average concentrations, such concentrations beginning to decrease in spring, with the photosynthesis becoming more intense.

River waters: for these waters, 10-year (2006–2015) averages of the respective annual average concentrations in the river basins of the White and Barents Seas were

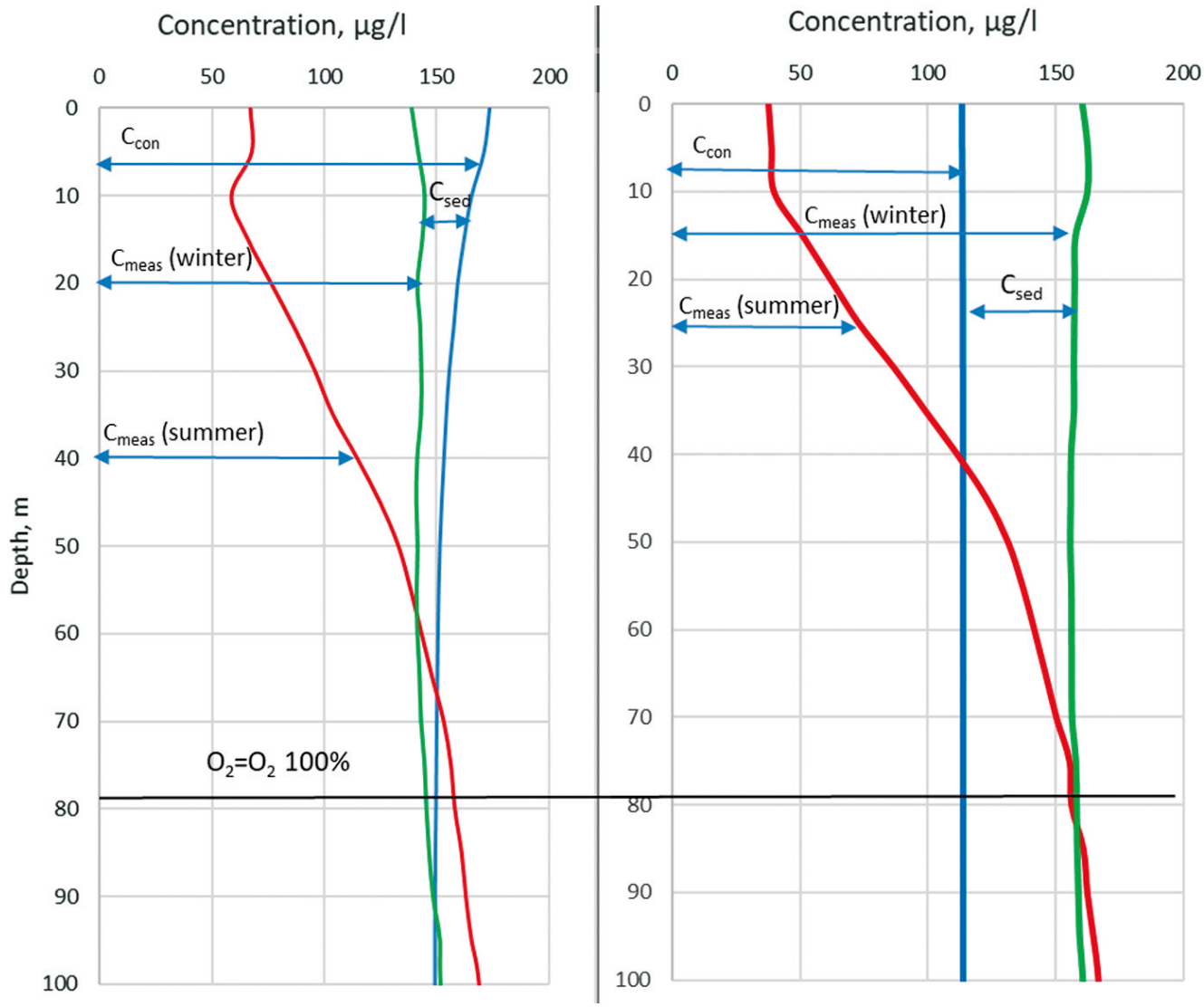

Fig. 1. An example of the vertical distribution of nitrogen-nitrate concentrations in one of the regions of the Barents Sea. The red line represents summer distribution; the green line shows winter distribution; the blue line shows conservative concentration; the black line is the horizon where dissolved oxygen saturation in the water decreases in summer to less than 100 %. Left, $C_{meas}(winter) < C_{con}$, indicating an outflow of the element related to the non-productive component; right, $C_{meas}(winter) > C_{con}$, indicating an inflow of the element related to the non-productive component.

taken, based on the yearbooks of surface water quality (Yearbook).

Ice: salinity and elements concentrations were based on the materials published in the book "The Seas of the USSR. The Barents Sea" (Terziev, 1991), such materials having been obtained as part of scientific research implemented on the "Otto Schmidt" icebreaker in 1980s.

The technique for calculating f_a, f_r, and f_i is explained below, in the hydrological block section.

Calculation of the non-conservative component values ($\Delta C_{non-con}$)

The value of the "non-conservative" component is the difference between the measured and the conservative values.

$$\Delta C_{non-conj} = C_{measj} - C_{conj}, \quad (5)$$

where j is the parameter considered (mineral phosphorus, silicon, nitrogen, or any other).

Then, if $\Delta Cj < 0$, the concentration of a particular nutrient is decreasing due to non-conservative factors (below, we will not use the $_{non-con}$ index).

Using equations 1–5, one can calculate total non-conservative concentration, which is a sum of both production and non-production components. Since the primary production is determined in a volume of water occupying a unit area, the values obtained must be integrated from the surface to the horizon where the concentration measured is equal to the winter concentration. As the lower limit of integration, let us take the maximum horizon where water saturation with dis-

solved oxygen changes from values above 100 % to values below 100 % in the course of the year. In this case, the integration limit should not exceed the maximum horizon where such change is observed, otherwise the values obtained will be underestimated. But, in order to avoid the influence of other processes, it is recommended to use a lower limit of integration that is close to the point indicated above. For each calculated point, the position of the horizon (***h***) where the value of water saturation with dissolved oxygen would cross the level of 100 % was determined. In different parts of the sea, this position varied from 40 m (or from the bottom layer) to 100 m.

For each month, the monthly average of C_{con} and C_{meas} integrated from the surface to the selected horizon ***h*** was calculated. The ***dh*** values are shown above.

$$Q_m^n = \int_0^h C_{meas}^n dh \text{ and } Q_c^n = \int_0^h C_{con}^n dh \qquad (6)$$

The index ***n*** indicates the month (1, 2, … 12).

For each month, the non-conservative component ΔQ^n was calculated as the difference between the values of the integrals Q_m^n and Q_c^n.

$$\Delta Q^n = Q_c^n - Q_m^n \qquad (7)$$

This value reflects total "non-conservativeness", i. e., the total change in the nutrient that is caused by the combination of the processes of photosynthesis and organic matter mineralization (the productive component) and the processes of biogenic matter exchange, both vertically and horizontally (the non-productive component). A positive value (+) indicates the total element consumption; a negative value (–) indicates the total element income. If the change in the nutrient in question depends only on the photosynthetic activity processes and the mineralization of the organic matter formed, then before the onset of photosynthesis this value will be equal to zero. If it is not equal to zero, this indicates an inflow or an outflow of the element caused by other processes, such as advection, exchange with underlying layers, etc. The minimum value of the ΔQ^n for the year, which is seen before the onset of photosynthesis (in different areas of the sea, this is usually February or March), will be the value of the non-productive component.

$$\Delta Q_{sed} = \min\left(\Delta Q^n\right) \qquad (8)$$

In this paper, we will assume that this value is constant throughout the year, but varies from region to region. If it is positive, then there is an outflow of the nutrient from the euphotic layer, and vice versa. In this case, the balance of the nutrient at the point can be expressed as:

$$Q_c^n - Q_{phyto}^n - \Delta Q_{sed} - Q_m^n = 0 \qquad (9)$$

The component that depends only on the photosynthetic activity and on the mineralization of the formed organic matter is calculated for each month using formula (9).

$$Q_{phyto}^n = Q_c^n - Q_m^n - \Delta Q_{sed} \qquad (10)$$

Formula (10) describes the change in the supply of a nutrient in the euphotic layer from month to month (n = 1, 2, 3 … 12). But, as was shown in some studies (Arzhanova and Zubarevich, 1995a; 1995b; 1997; Nesvetova, 2003), this value decreases due to the return of the element to the marine environment as a result of its regeneration. Then, taking into account the regeneration of the nutrient, equation (10) can be written as follows:

$$Q_{phyto}^n = Q_c^n - \left(Q_m^n - Q_r^n\right) - \Delta Q_{sed}, \qquad (11)$$

where Q_r^n is the increase of the element reserve due to the element's remineralization.

In the primary production estimates performed by Arzhanova N. V. for the Sea of Okhotsk, the value of silicon regeneration was taken to be 50 % of the amount already consumed by phytoplankton. In that study, the regeneration was estimated for each region separately. This was made by estimating the regeneration rates of the elements by the rate of their stock replenishment at such points of time when photosynthesis had either stopped or was extremely slow, and the replenishment of the nutrients stock from the underlying layers was hindered by the vertical water density gradient that had not yet been destroyed. As will be shown below, this usually happens in October or November. In formula (12) $\left(Q_{phyto}^{n-1}\right)$ is the value based on which the element regeneration for the month ***n*** is determined.

$$Kj = \frac{\left[\left(QP_{phyto}^{n-1}\right) - \left(Q_{phyto}^n\right)\right]}{\left(Q_{phyto}^{n-1}\right)} \qquad (12)$$

The coefficient *Kj* for the area in question is determined using the descending part of the curve (Fig. 2), where the decrease of Q_{phyto}^n from month ***n-1*** to month ***n*** is the largest in the year. The regeneration coefficient is assumed to be constant in the area for the whole year, but the absolute value of regeneration will change from month to month since it is defined based on the amount of the elements already consumed by that time. Of course, this value will depend on the water temperature and the species composition in the phytoplankton; but an examination of such dependencies and their application will be considered at the next stage of this method improvement.

As a result, the final amount of nutrients consumption by photosynthesis in the month ***n*** will be determined by the formula:

$$Q_{phyto}^n = Q_c^n - Q_m^n - \Delta Q_{sed} + \left(Q_{phyto}^{n-1}\right) * Kj \qquad (13)$$

ECOLOGY

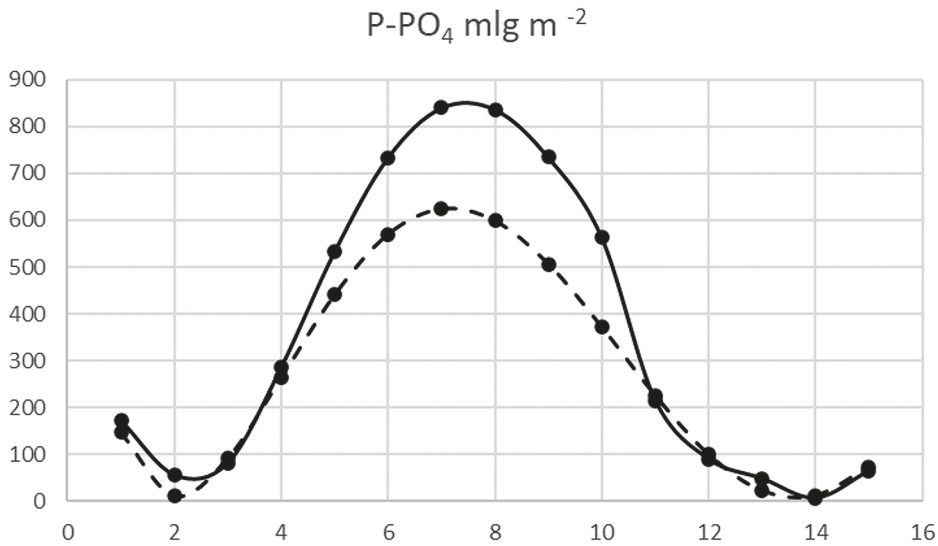

Fig. 2. An example of the final assessment of the element consumption annual cycle. The dotted line shows consumption without remineralization, the solid one shows consumption assessment taking remineralization into account (Eq. 12).

In Fig. 2, ***n*** can take values that correspond to the descending part of the graph (usually, n is 10 or 11). In this particular case, ***n = 11***, November; then ***n – 1*** is October. (***Kj*** = (380–220)/380 = 0.42).

Calculation of primary production

Today, the transition from the nutrients' consumption to primary production, i. e., to carbon consumption, in most cases is performed using the average stoichiometric Redfield — Richards ratios, namely, in the molar form, C : Si : N : P = 106 : 23 : 16 : 1 (Redfield 1934; 1958; Richards, 1958). But applying these ratios to phytoplankton with various species compositions can lead to major errors. Thus, the ratios of the elements mentioned differ significantly across various dominant groups of the plankton. For example, the C : P ratio change in the phytoplankton differs by 37 % between diatom and peridinium plankton, C : N ratio change — by 24 %, and C : Si ratio change — by 15 times (Table 2). It is especially important to account for the C : Si ratio change variations, since, as was mentioned above, silicon production calculation reflects total production (NCP_{Si}).

Table 2. Relative chemical composition in phytoplankton systematic groups (Sverdrup, Johnson, and Fleming, 1942 from Bordovsky and Ivanenkov, 1979)

Plankton	C	Si	N	Ph (phosphorus)
Diatom	100	93.0	18.2	2.7
Peridinium	100	6.6	13.8	1.7

In the present study, we attempted using individual stoichiometric ratios. Here, we assumed that all phytoplankton consisted of two systematic phytoplankton groups only, namely diatoms and dinoflagellates. This assumption, too, introduced an error into the calculations. But according to the Biological Atlas of the Barents Sea (Melling and Moor, 1995), in an evaluation of the entire Barents Sea based on an analysis of 1000 samples, the average sum of the biomasses of these two phytoplankton groups was 94 %. That is, the biomass of other phytoplankton systematic groups comprises 6 % only. According to the results of some expeditionary field studies, the total biomass of these two groups in the Barents Sea comprised as much as 99 % (Pautova et al., 2019).

The observed measured (real) stoichiometric ratio of carbon to one of the nutrients will be equal to the ratio of the amount of carbon to the amount of silicon, nitrogen, or phosphorus (index *J*) involved in photosynthesis:

$$k_J = \frac{\left(Q^n_{phyto}\right)_C}{\left(Q^n_{phyto}\right)_J} \qquad (14)$$

The numerator is the amount of carbon involved in photosynthesis; the denominator is the amount of the nutrient *J* involved in photosynthesis.

Since we assume that all phytoplankton consists of two systematic groups, namely diatoms and peridiniums, we can calculate k_J using the data on the phytoplankton relative chemical composition according to H. Sverdrup (Bordovsky and Ivanenkov, 1979), as represented in Table 2.

$$dk_d + pk_p = k_j, \qquad (15)$$

where: d = relative contribution of carbon from the diatom plankton biomass in the total primary production; p = relative contribution of carbon from the peridinium

plankton biomass in the total primary production; k_d and k_p = stoichiometric ratios of carbon to *j*-th nutrient in diatom and peridinium phytoplankton, respectively, calculated based on Table 2.

Since we assume that there are only 2 systematic groups of phytoplankton:

$$d + p = 1 \tag{16}$$

k_J: are stoichiometric ratios calculated based on nutrients consumption in photosynthesis. *Index j* is Si, N, or Ph (phosphorus). In this study, we are using ratios of Si/Ph and Si/N for further calculations.

$$k_{Si/Ph} = \frac{\left(Q^n_{phyto}\right)_{Si}}{\left(Q^n_{phyto}\right)_{Ph}} \tag{17}$$

Using equations 14–17, it is easy to calculate *d* and *p*.

$$d = \frac{k_{Si/Ph} - k_P}{\left(k_d - k_p\right)} \tag{18}$$

In this case, k_d and k_p are the *Si/Ph* ratios in diatom and peridinium planktons, calculated based on Table 2. The value of $k_{Si/Ph}$ was calculated using formula 17. Equation (19) describes the calculation of the current, or individual stoichiometric ratio of carbon to an element after having calculated *d* and *p*.

$$dk_d + pk_p = \frac{\left(Q^n_{phyto}\right)_C}{\left(Q^n_{phyto}\right)_J} \tag{19}$$

In the end, primary production is calculated using equation 19 with known values of *d* and *p*.

$$\left(Q^n_{phyto}\right)_C = \left(Q^n_{phyto}\right)_j * \left(dk_d + pk_p\right) \tag{20}$$

In equations 19–20, index C is carbon consumption (primary production). In this case, it corresponds to the (NCP_{Si}) value, if calculation for silicon was performed (*j*=*Si*, k_d and k_p being stoichiometric ratios of carbon to silicon, calculated based on Table 2); or to (NCP_N) value in case of a calculation for nitrogen (*j* = *N*, k_d and k_p being stoichiometric ratios of carbon to nitrogen calculated based on Table 2).

Calculation technique for f_a, f_r, and f_i (hydrological block)

To calculate the conservative concentration (Eq. 3), it is necessary to know the composition of the sample in question in terms of various water types (Atlantic, river, and ice waters). Data from the NODC (Boyer et al., 2018) and NASA (Schmidt. Bigg, and Rohling, 1999) public databases were used in the present study.

Calculation of f_a, f_r, and f_i is carried out based on salinity and the isotopic parameter value, taking into account corrections that are due to the predominance of ice formation over ice melting (fi < 0). To estimate the relative volumes of Atlantic, river, and ice waters, a three-component system of mixing equations was used in various studies (Bauch et al., 2003; Bauch, Schlosser, and Fairbanks, 1995; Bauch and Cherniavskaya, 2018; Dubinina, Kossova, Miroshnikov, and Fyaizullina, 2017; Dubinina, Miroshnikov, Kossova, and Shchuka, 2019; Melling and Moor, 1995; Namyatov and Semeryuk, 2019; Namyatov, 2021; Ostlund and Hut, 1984; Semeryuk and Namyatov, 2018; etc.):

$$\begin{gathered} fa \times Sa + fr \times Sr + fi \times Si = Smeas\,, \\ fa \times Ia + fr \times Ir + fi \times Ii = Imeas\,, \\ fa + fr + fi = 1\,, \end{gathered} \tag{21}$$

where S_r is salinity of "pure" river waters, which is always zero (S_r = 0) (psu); S_i is sea ice salinity (psu); S_a is salinity of "pure" Atlantic waters (psu); I_a is the value of the isotope parameter $\delta^{18}O$ for "pure" Atlantic waters (‰); I_r — that for "pure" river waters (‰); I_i — for ice waters (‰); f_a, f_r, and f_i are the portions of Atlantic, river, and ice waters, respectively (%); S_{meas} is the resulting (measured) water salinity (psu); I_{meas} is the resulting (measured) value of the isotope parameter $\delta^{18}O$ (‰). Such system of equations can only be used where the ice-melting process predominates ($fi > 0$) (Dubinina, Miroshnikov, Kossova, and Shchuka, 2019). If ice formation prevails ($fi < 0$), the equations system (21) is supplemented by two more equations (Namyatov, 2021):

$$fa^w = fa - k\,x|fi|/(1 + k) \tag{22}$$

$$\begin{gathered} fr^w = fr - |fi| + k\,x\,|fi|/(1 + k) \\ fa/fr = k \end{gathered} \tag{23}$$

The use of the equations system (21) in the case of ice formation predominance is not entirely legitimate, which was for the first time shown in a study by Dubinina E. O. et al. (2019); but the paper proposed a calculation technique for river waters only.

In this case, fa^w and fr^w reflect the portions of Atlantic and river waters, respectively, in the subglacial water layer (Namyatov, 2021). *fa* and *fr* designate the content of Atlantic and river waters, respectively, calculated using the equations system (21). The final salinity and isotope parameter values to be used in the calculations are shown in Table 3.

Data

For both the hydrological and ecosystem blocks, data from the NODC oceanographic data bank and from WOA18 were used (Fig. 3), namely the data on salinity, phosphorus-phosphate, nitrogen-nitrate, and silicon.

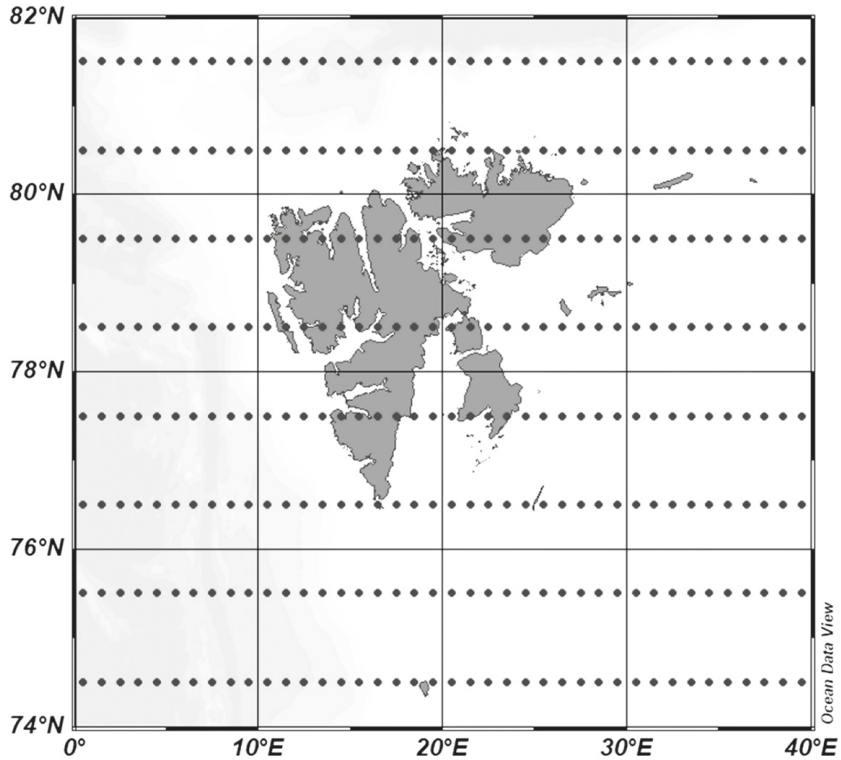

Fig. 3. Grid nodes positions in the WOA18 oceanographic atlas (Boyer et al., 2018).

Table 3. End-Member Values Used in Mass Balance Calculations

Ia (‰)	Ir (‰)	Ii (‰)	Sa (psu)	^{3}Si (psu)
0.354[3]	–14.23[4]	[5]Values on he surface + 1.96 ‰	35.135[1]	5.86[2]

1. Defined by the author based on NODC (Boyer & 2018 & 2018) data for the Barents Sea waters as the median value for 10–17E, 71–75N square in the 150–250 m layer, in February;
2. Calculated based on the ice salinity definition 288 provided in the book "The Seas of the USSR. The Barents Sea" (Terziev, 1991);
3. Defined by the author based on the database (Schlitzer, 2021) data for this square (see p. 1);
4. Weighted average for the Kola, Severnaya Dvina, Pechora, and Pinega rivers, taking annual runoff into account, based on the data from co-author Tokarev I. V.;
5. Determined by the authors using joined determination of $\delta^{18}O$ in the sea water under ice and in the ice in the Barents Sea (1.81 ± 0.34 in 6 samples (see additional information), and combined with the data from Melling and R. M. Moore (Melling and Moor, 1995) (2.09 ± 0.38 in 7 samples) for the Beaufort Sea.

In the atlas, the data are given as dataset grids, with 1° increment in both latitude and longitude, at standard horizons of 0, 5, 10, 15, 20, 25, 30, 35, 40, 45, 50, 55, 60, 65, 70, 75, 80, 85, 90, 95, 100, 125, 150, 175, 200, 225, 250, 275, 300, and so on. In this study, we used average monthly values of the parameters above (Boyer et al., 2018).

In this study, data on $\delta^{18}O$ and salinity from public databases were used. These data were collected between 1972 and 2008 and published on the NASA (Schmidt, Bigg, and Rohling, 1999) and NODC (Boyer et al., 2018) websites. The list of the data used was provided in (Namyatov, 2021). In addition, the results of research undertaken in 2014 were used. The error of $\delta^{18}O$ measurement was 0.03–0.07 ‰ in the studies conducted in 1993–1995 and 0.1–0.2 ‰ in the studies conducted before 1989 (Bauch et al., 2011). Finally, the present study used data from the parallel determination of $\delta^{18}O$ in the ice and in the under-ice water layer conducted as a part of an expedition aboard the R/V Dalnie Zelentsy in 2021 in the Barents Sea. The contents of stable isotopes $\delta^{18}O$ were determined using a Picarro L2130-i laser analyzer (manufactured in 2021) at the Resource Center "X-ray Diffraction Research Methods" of the St. Petersburg State University Science Park. The standards used are USGS50 ($\delta^{18}O$ = +4.95 %), USGS45 (δ18O = –2.238 %), USGS46 (δ18O = –29.80 %). The measurement error was ±0.025 % for $\delta^{18}O$ (Table 3).

Since we are using data on nutrients and salinity at the grid points, we need to know the value of the isotope parameter corresponding to each salinity value; but such data are unavailable. Many studies have shown that the

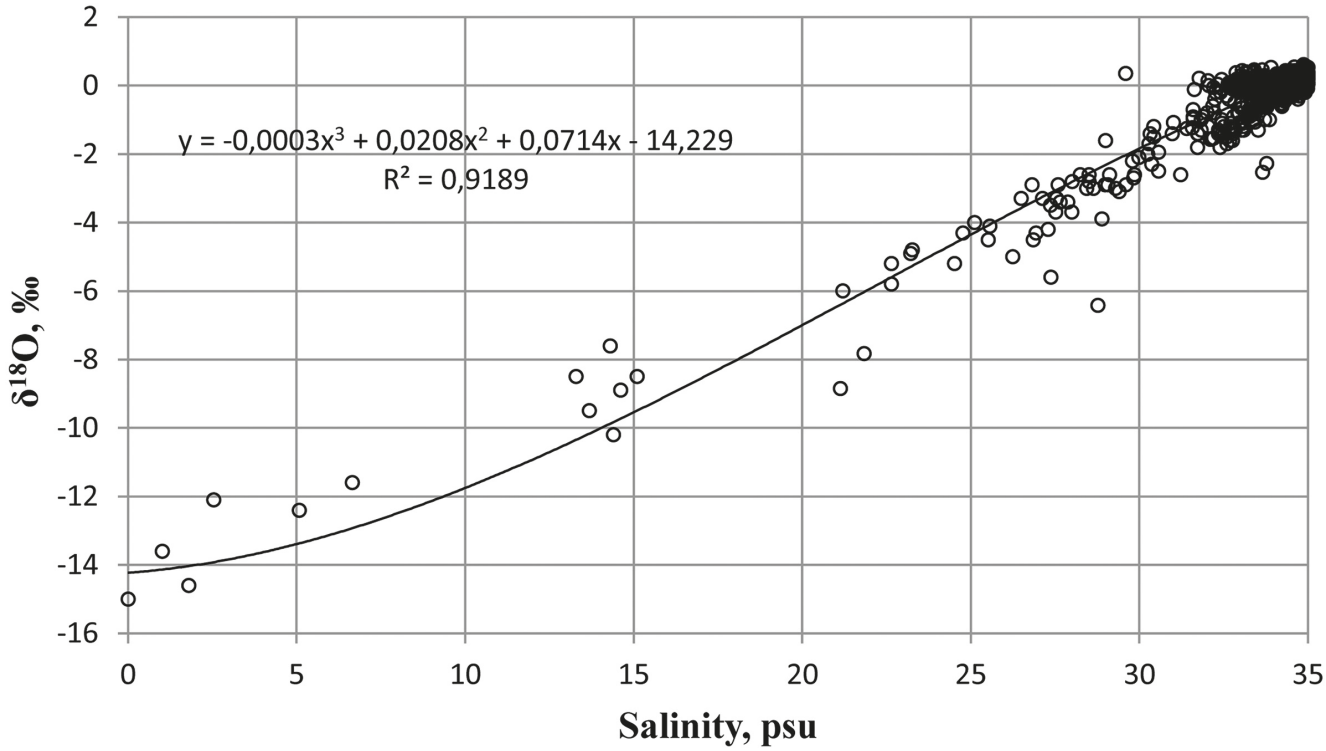

Fig. 4. The equation of the relationship between salinity (psu) and $\delta^{18}O$ (‰) for the Barents Sea.

dependency between salinity and $\delta^{18}O$ is characterized by a correlation factor close to 1. The generalized dependency obtained from the results of 2182 measurements at 319 stations in the Barents Sea, based on the results of studies conducted by various groups of authors, is presented in (Namyatov, 2021) (Fig. 4).

In this case, the correlation factor is close to 1 (R2 = 0.91). Since this graph represents all the data, regardless of the season and sampling horizon, we assume that the resulting relationship equation is applicable to all salinities, regardless of whether the $\delta^{18}O$ value was measured along with the salinity or not. This hypothesis was tested by dividing the series randomly into two subseries, with 1100 values each. The equation of the relationship between salinity and $\delta^{18}O$ was calculated based on the data from the first series. Then, applying this equation to the second series, $\delta^{18}O$ values were calculated based on the salinity values. Further, the calculated and measured values of $\delta^{18}O$ were compared with each other. The significance of linear regression between the measured and calculated $\delta^{18}O$ values was tested using Fisher's f-test. Student's t-test was used to check the equality of the mean values in the two samples. For both tests, the significance level was less than 0.05. Therefore, our assumption is valid, and it is possible to calculate the $\delta^{18}O$ value for each salinity value even outside of the area of these parameters' mutual determination. In this study, the values of the $\delta^{18}O$ isotopic parameter for each salinity value were calculated using the equation presented in Fig. 4.

All data were collected and integrals (Eq. 6) calculated using the Ocean Data View software package (Schlitzer, 2021).

Statistical processing, including the calculation of linear trends, testing the significance of linear regression (Fisher's F-test), and checking the equality of the means in two samples (Student's t-test), were carried out using the EXCEL software package.

In total, for this area, the calculations were performed for values at ~285 grid points (Fig. 3). All calculations for the equations 1–7, including equations 21–23, as well as the regression equation in Fig. 4, were carried out for each month at each calculated point and at each horizon (as presented above, from 10 to 25 horizons). Further, the integration results obtained by formulas 6 and 7 were averaged for regions of 10° in longitude (starting from 0° E) and 2° in latitude (from 68° N). About 20 grid nodes were located in each square. There were 15 squares in total. Further calculations were carried out for each square.

Results and discussion

Verification of the obtained results

An evaluation of primary production in the waters surrounding the Svalbard archipelago was demonstrated in Reigstad et al., 2011. In that study, primary production was calculated based on two models: a hydrodynamics

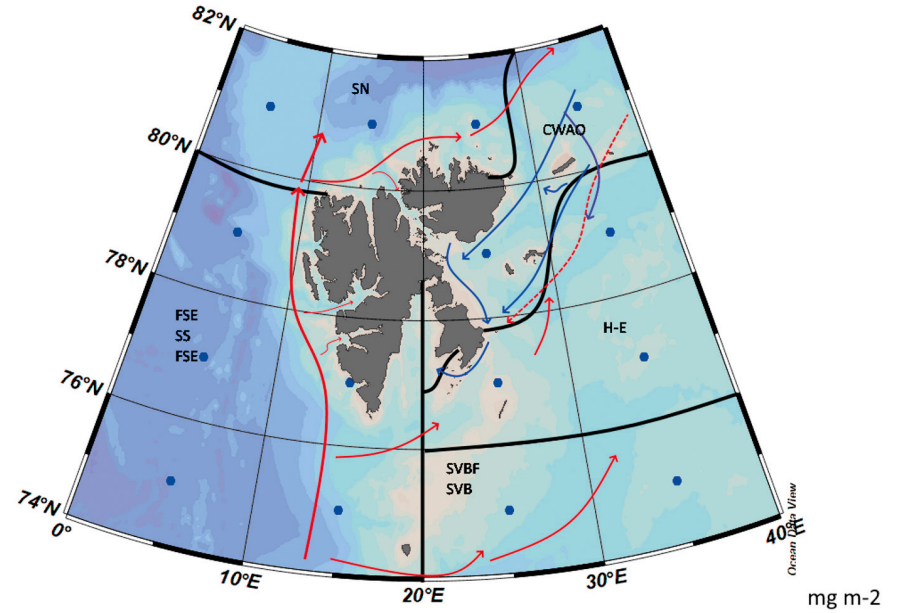

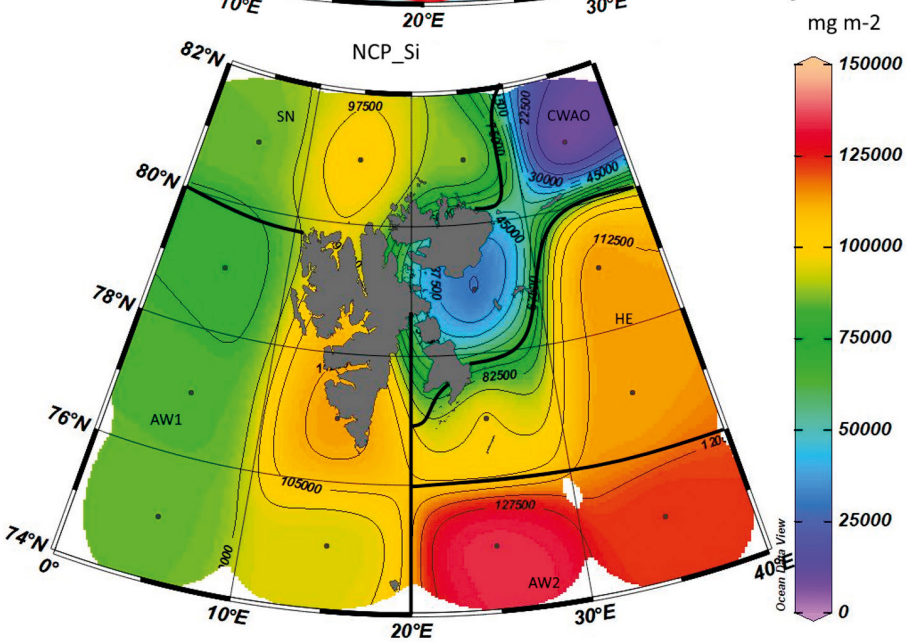

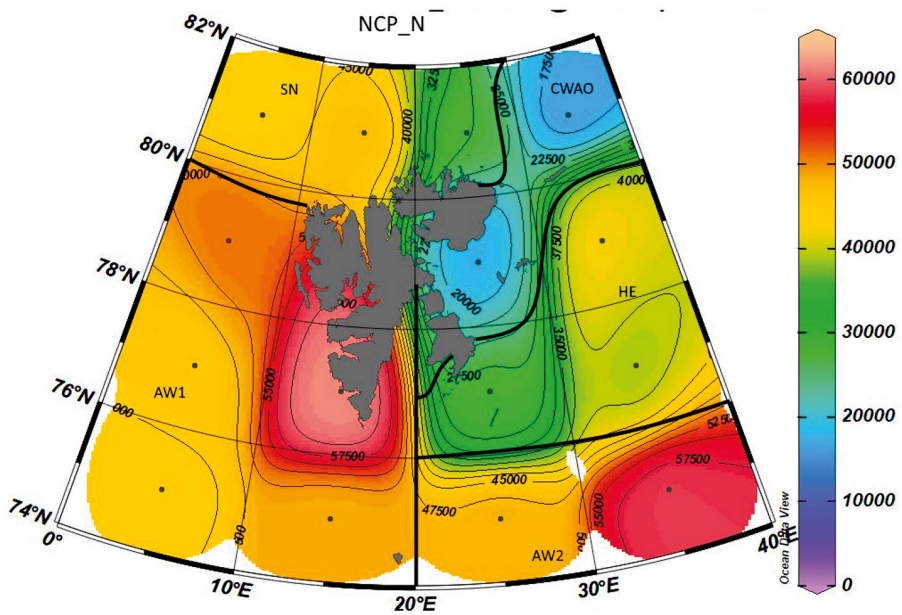

Fig. 5. Location of cluster boundaries (black lines); general diagram of Atlantic water influx (solid red lines); recurrent Atlantic water influx (red dashed lines); cold waters of the Arctic Ocean influx (blue lines) (Moiseev, Zaporozhtsev, Maximovskaya, and Dukno, 2019); provinces names and acronyms are used according to (Reigstad et al., 2011).

Table 4. Average values of primary production (NCP_{Si}) and standard deviations in the regions of the Svalbard (gCm^{-2})

Reigstad et al., 2011		* Present study		
Region**	Average ± sd	Average ± sd	max	Cluster name
Svalbard waters province	100 ± 7	91 ± 33	138	SW
Western Svalbard Shelf (SS)	106 ± 8	90 ± 8	100	AW1
West Spitsbergen Current (WSC)	134 ± 8			
Fram Strait East (FSE)	108 ± 6			
Svalbard Bank Frontal System (SVBF)	112 ± 8	131 ± 9	138	AW2
Svalbard Bank (SVB)	113 ± 10			
Svalbard North (SN)	54 ± 10	90 ± 4	96	SN
Hindlopen Strait (H-E)	67 ± 12	108 ± 9	114	HE
Cold waters of the Arctic Ocean (CWAO)	no	19 ± 1.4	20	CWAO

Notes: * — primary production accumulated during August and September; ** — provinces names and acronyms are used according to (Reigstad et al., 2011).

and an ecosystem one. The hydrodynamics model is a large-scale one, with horizontal mesh points located at 20 km from each other, and with a nested model resolution of 4 km. "The ecosystem module includes nitrate, ammonium, silicate, diatoms, flagellates, microzooplankton, bacteria, heterotrophic nanoflagellates, fast sinking detritus, slow sinking detritus and two mesozooplankton groups Calanus finmarchicus and Calanus glacialis".

One cannot expect the results of the present study to be totally consistent with those of the study described above because of the differences in horizontal resolution, time interval of the input data, etc. Still, some general patterns should be visible. In the abovementioned study, the authors distinguished between 7 provinces in the water area around the Svalbard archipelago, according to PP values in these provinces. In this case, for the purposes of verification, one should compare province boundaries location and average PP values in each province (Table 4, Fig. 5).

For the purposes of verification, the results were subjected to cluster analysis based on classification by Ward's method and Euclidian distances (Ward, 1963). All the input data were rated. The input data comprised *temperature, salinity,* f_i, NCP_{Si} and NCP_N.

Although our calculations were characterised by a much lower horizontal resolution, we were able to reveal 4 clusters. According to our analysis results, H-E and SN provinces were combined to form a single cluster. But, as these provinces are separated by the Svalbard archipelago and located far from each other, we will consider them as two separate clusters. The boundaries of the 4 clusters revealed by us practically comprised the waters of the 7 provinces described in the article above. We revealed an additional province, namely the Cold waters of the Arctic Ocean (Table 4, Fig. 5).

As concerns the average PP values across the whole water area examined, the results were rather consistent. Another common pattern was present in both cases, namely that the highest PP values were observed in the waters that were comprised mostly of Atlantic water, while the lowest ones were observed in the water's incoming from the Arctic Ocean.

The PP values were consistent between the two studies in the regions where the water consisted mostly of incoming Atlantic water, namely SS, WSC, FSE, SVBF, and SVB (Table 4). In the regions that featured more mixing of Atlantic and Arctic Ocean water (provinces SN and H–E), the PP values in our study were around 2 times higher than in Reigstad et al. (2011). The minimum PP values (~20 gCm^{-2}) were observed in the waters incoming from the Arctic Ocean.

This allows to conclude that the PP evaluation technique shown in the present study, while providing results comparable to those of other evaluation techniques, possesses some advantages.

Discussion

The PP values (NCP_{Si}, NCP_N, and NCP_P) obtained using this technique were the ultimate result of intermediate parameters evaluation and analysis. Analysing the intermediate parameters allowed to conceive the mechanisms or interactions existing in a system that can be divided into a hydrological, a hydrochemical, and a hydrobiological blocks. The hydrological block concerns water composition in terms of Atlantic, river, and ice water masses (f_a, f_r, and f_i, respectively).

The intermediate parameters of the hydrochemical block were the measured nutrient reserve (Q_m), conservative reserve (Q_c), nutrient inflow/outflow in the euphotic layer (Q_{sed}), nutrient remineralisation coefficient (K_J). Using these parameters allowed to obtain true stoichiometric ratios C : Si : N : P. It also provided for a possibility to calculate relative nutrients reserves/consumption R_P, R_N, and R_{Si}, that is relative consumption of phosphorus, nitrogen, and silicon (%), respectively, similarly to water saturation with dissolved oxygen.

The intermediate parameters of the hydrobiological block were relative biomasses (in terms of carbon) of diatom (d) and peridinium (p) planktons; later, these are to be corrected and complemented with total relative biomass of the remaining phytoplankton.

An analysis of the hydrochemical regime that would consider all the parameters above is a separate

Table 5. Values of some of the intermediate parameters used in PP calculation (August — September)

Province	[1]C : SI : N : P	[2]R_P (%)	[3]R_N (%)	[4]R_{Si} (%)	[5]p (%)	NCP_{Si} gC m^{-2}	NCP_N gC m^{-2}
SW	52.0 : 17.7 : 8.3 : 1	48 ± 10	69 ± 13	73 ± 15	0.66 ± 0.25	91 ± 33	41 ± 13
AW1	54.8 : 9.4 : 7.3 : 1	45 ± 6	59 ± 11	60 ± 11	0.82 ± 0.12	90 ± 8	49 ± 8
AW2	53.3 : 12.3 : 7.8 : 1	40 ± 6	71 ± 10	60 ± 11	0.73 ± 0.13	131 ± 9	53 ± 7
SN	55.2 : 27.6 : 12.5 : 1	44 ± 11	61 ± 8	82 ± 8	0.81 ± 0.04	90 ± 4	40 ± 9
HE	46.5 : 16.0 : 9.3 : 1	56 ± 5	77 ± 4	88 ± 3	0.60 ± 0.03	108 ± 9	40 ± 7
CWAO	37.0 : 40.6 : 7.0 : 1	49 ± 5	64 ± 4	91 ± 2	0	19.0 ± 1.4	17.0 ± 0.6

Notes: [1] — stoichiometric ratio (typically, Redfield — Richards stoichiometric ratio is used, which is C : Si : N : P = 106 : 23 : 16 : 1 in molar form, or 41.1 : 20.9 : 7.2 : 1 in terms of mass); [2, 3, 4] — relative consumption of nutrients — phosphorus, nitrogen, and silicon, respectively; [5] — relative biomass of peridinium plankton (in terms of carbon).

task which could be described in an additional paper or papers.

The results obtained using the present technique allowed for a new view on the analysis of the hydrochemical and, to some extent, hydrobiological (phytoplankton) regimes of marine ecosystems. Values of some of the intermediate parameters above are shown in Table 5.

By now, a lot of data on salinity and nutrient concentration values have been accumulated; this allows the present technique to be used to assess the characteristics of PP values variations in the water area examined. As concerns the waters surrounding the Svalbard archipelago, the distribution of PP values in this area is shown in Fig. 5.

It is possible to divide the waters of this area into three groups by their origin: Atlantic waters (AW1 and AW2), cold waters of the Arctic Ocean (CWAO area), and mixed waters (areas HE and SN). Atlantic waters are comprised of the Fram Strait and the West Spitsbergen Current waters (cluster AW1) and South Spitsbergen Current waters (cluster AW2).

The main hydrological forces influencing the development of phytoplankton community in this region are the warm waters of the South Spitsbergen Current, as well as the existence of a temporary ice edge. In the waters of this area, the highest PP values were observed. The lowest, near-zero values were observed in February (Fig. 6). At the same time, as compared to February, higher primary production values of 37 gCm^{-2} were observed in January. This PP seemed to be the residual non-mineralised part of the PP left from the previous photosynthesis cycle. Based on the nutrient concentration changes, the photosynthesis onset in this region may be registered in March. Average primary production (NCP_{Si}) values in the region are 12 gCm^{-2}. At this time, photosynthesis is driven by nutrients reserves established during winter. The NCP_{Si} to NCP_N ratio of 1.36 is not very large. In spring, the pelagic zone contains a group of species that is present during this season only: *Chaetoceros socialis, Fragilariopsis oceanica, Navicula pelagica, N. vanhoeffenii, Nitzschia frigida, Thalassiosira hyalina, Porosira glacialis, Phaeocystis pouchetii*. These are typical species of the early-spring stage of the phytoplankton succession cycle in the Barents Sea (Makarevich, Druzhlova, 2010). In spring, diatoms comprise about 90 % of total biomass, but in some years *Phaeocystis pouchetii* (class Prymnesiophyceae) can reach a high rate during its bloom peak, up to 95 % of the total plant community biomass.

The highest accumulated primary production was observed from August to October. In this period, average water temperature across the euphotic layer is 3.32 °C, while average total primary production is 131 ± 9 gCm^{-2}. Nitrogen recycling rates in these months are the highest, which is marked by an increase of NCP_{Si} to NCP_N ratio up to 2.45. Across the whole area of this province, located to the south of the archipelago, an algocenosis of a uniform taxonomic composition has developed, with a core comprised of species with an all-year vegetation period (Makarevich and Oleinik, 2017). The structure of the pelagic algal flora in the region in terms of species-level taxons is dominated by diatoms (around 55 %) and dinoflagellates (around 40 %). The remaining nutrients reserves do not serve as a limiting factor for photosynthesis, comprising 60 % in case of phosphorus, 40 % for silicon and 30 % for nitrogen (Table 5). The relative biomass of peridinea in these waters, calculated based on nutrients consumption, at the time when photosynthesis reaches its highest rates was 0.73 ± 0.13. Therefore, calculated relative biomasses of diatoms are within 20–40 %.

Later, in November, the photosynthetic activity decreases and drops dramatically (NCP_{Si}) to 58 ± 25 gCm^{-2}, while NCP_{Si} to NCP_N ratio decreases to 1.87. Mineralisation processes flow at a slow rate, and residual primary production in December is 40 ± 15 gCm^{-2}. NCP_{Si} to NCP_N ratio is 1.80 in December and as low as 1.27 in January. By February, PP drops to zero, which, obvious-

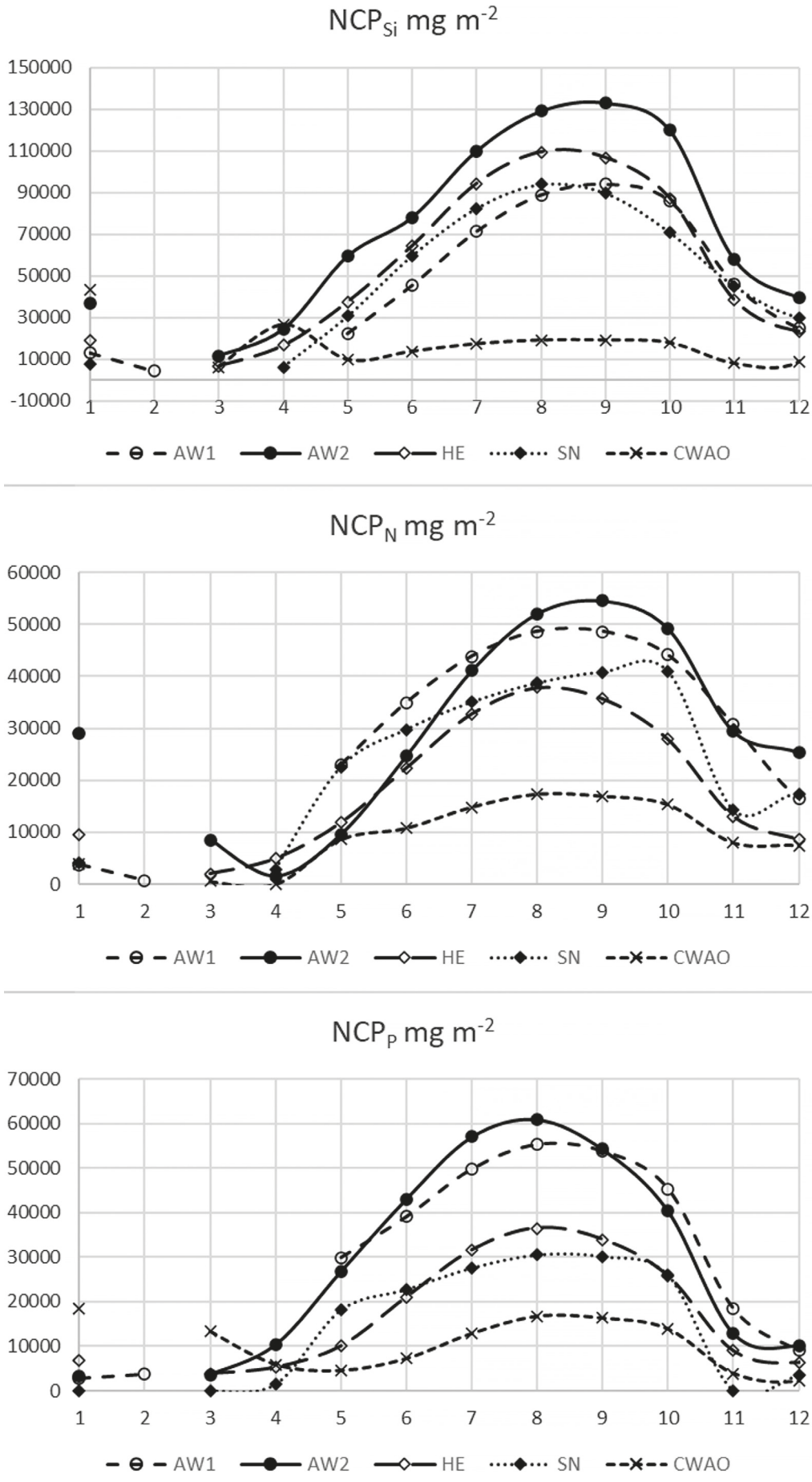

Fig. 6. Annual cycle of Primary Production change in terms of silicon, nitrogen, and phosphorus in every region

ECOLOGY

ly, is not only due to the organic matter mineralisation in the surface layer, but also to a vertical exchange that happens after vertical density gradients have vanished.

In winter, peridinea algae start dominating in terms of biomass, but, being extremely low (compared to the total vegetation period), it causes no significant influence on the structure of total annual biomass of primary organic matter synthesised in the pelagic zone.

The waters of the Fram Strait surround the western and northern parts of the archipelago and are characterised by an inflow of warm Atlantic water brought by the West Spitsbergen Current. The West Spitsbergen Current is a warm surface current going along the western shores of the Svalbard archipelago as a continuation of the Norwegian Current. It bears the warm Atlantic waters into the Arctic Basin, close to the shore of the Western Spitsbergen Island. Its water temperature is 2–4 °C in summer and 1–3 °C in winter. Salinity is 34.9 ‰. The current velocity at the surface is 20–30 cm/s. To the north of the Western Spitsbergen Island the current submerges, forming the warm intermediate waters of the Arctic Ocean (Great Russian Encyclopaedia). Annual cycle of PP values is nearly the same as in the South Spitsbergen Current, except that the highest PP values are 30 % lower, namely 90 ± 8 gCm^{-2}. NCP_{Si} to NCP_N ratio is also somewhat lower during this time, 1.95, which points to a somewhat slower organic matter mineralisation, although average water temperature in the euphotic layer is in fact 4.42 °C, that is 1 °C higher.

The West Spitsbergen Current causes advection of warm Atlantic water that plays an important role in the colonisation of Arctic surface waters by phytoplankton cells; this fact and the absence of an ice edge shape the structure of pelagic algocenosis in this province (the waters of the Fram Strait) in terms of taxonomy. In the waters of this region, the peridinea algae reach the highest diversity in terms of species; their contribution to total microalgae biomass during summer, autumn, and spring is also the largest (above 60 %). The dominant group includes the following peridinea algae: *Amphidinium fusiforme, Ceratium arcticum, Dinophysis acuminata, Gyrodinium fusiforme, Gyrodinium lacrima, Protoperidinium pellucidum, Katodinium glaucum;* diatoms: *Thalassiosira* spp., *Chaetoceros borealis, Nitzschia frigida;* and cryptophytes: *Plagioselmis* sp., *Teleaulax acuta*. Relative biomass of peridinea in these waters, calculated based on the nutrients consumption when the photosynthesis rate is the highest, is 0.82 ± 0.12. The remaining nutrients reserves in these waters do not serve as a limiting factor for photosynthesis, comprising 55 % for phosphorus, 40 % for silicon, and 40 % for nitrogen (Table 5). Relative contribution of peridinea, being very high in these waters, allows to compare calculated stoichiometric ratios of nutrients consumption with the data on their share in the peridinium plankton. According to Table 2, the stoichiometric mass ratio for peridinium plankton is 100 : 6.6 : 13.8 : 1.7. In the water area discussed, this ratio, calculated based on the nutrients consumption, is 100 : 17.2 : 13.3 : 1.8. This resulting ratio is rather close to that from the table, but the proportion of silicon is 2.6 times higher. The reason might be that Peridinea do not constitute 100 % of the plankton, diatom algae comprising an average of 18 %.

CWAO province is adjacent to the north-eastern part of the archipelago and expands further into the sea to the north-east. Most of the year, this province is either covered with ice or is featured by seasonal ice drift, which definitely impacts the structure and production of its pelagic algocenosis. The annual cycle of PP variation almost copies that of the Atlantic waters, the only difference being that its maximum value of 19.3 ± 1.4 gCm^{-2} is 6.8 times lower than in the South Spitsbergen Current waters.

The hydrochemical regime of the waters in this province is distinguished by a low rate of organic matter recycling. NCP_{Si} to NCP_N ratios from May to December vary within a range from 1.0 to 1.2. Figures in Table 5 reflect this phenomenon, providing a good explanation thereof. Almost 100 % of the algocenosis is comprised of diatoms, whose silicon-rich skeletons and shells decay very slowly in the dead algae. Low water temperature of an average of 0.11 °C in the euphotic layer in August and September also supports this. As diatoms comprise nearly 100 % of the algocenosis ($p = 0$), silicon reserves are consumed faster, because C : Si mass ratio in these algae is 1.07, compared to 15.15 in peridinium plankton (Table 2). Silicon being consumed almost fully (with a remainder of 8 %), phosphorus and nitrogen reserve rates are 50 and 35 %, respectively. Should the algocenosis composition be different, for instance with a portion of dinoflagellates, nutrients would have been consumed more evenly, with a higher PP value. The results obtained were confirmed by immediate measuring of phytoplankton parameters. Major primary producers of the pelagic zone in this area of the Barents Sea are the diatoms that create most of the production potential (being a major contribution to the integral biomass) within the whole vegetation period. Even though at some succession stages peridinea may show a higher species diversity, diatom algae almost always dominate in terms of number and biomass. The species that dominate this region are: *Chaetoceros concavicornis, Chaetoceros diadema, Gyrodinium lachryma/fusiforme, Protoperidinium depressum*.

The results above are unique in that they allow to obtain "true" stoichiometric ratios for diatom phytoplankton in the field. This allows both to verify the calculation technique and to compare the data on nutrients content in the phytoplankton with those obtained by H. Sverdrup as early as in 1942. While Table 2 shows a C : Si : N : P ratio of 100 : 93 : 18.2 : 2.7 in diatoms, according to the data obtained, this ratio is 100 : 109.7 : 18.9 : 2.7. The

ratios are rather close to each other. Nevertheless, calculated silicon consumption is still somewhat higher than that in the Table, namely 1.17 times higher.

As was mentioned above, based on the cluster analysis, the waters of the HE and SN provinces were combined into one cluster, although the provinces are located at a rather long distance. This points to the fact that these waters share the way their features had developed, driven by the incoming Atlantic waters and cold Arctic Ocean waters. These waters bear the characteristics of both types of water.

Average NCP_{Si} in the HE province at the highest rate of photosynthesis was 108 ± 9 gCm^{-2}, while in the SN province it was 90 ± 4 gCm^{-2} (in August — September). In the water area of the HE province, where South Spitsbergen Current waters interact with cold Arctic Ocean waters, diatoms contribute 40 % of the total phytoplankton biomass (by carbon), while relative silicon consumption at a rate of 88 ± 3 % is rather high. In the water area of the SN province, where West Spitsbergen Current waters interact with cold Arctic Ocean waters, diatoms contribution to the total phytoplankton biomass (by carbon) is 2 times lower, namely 20 %, relative silicon consumption being somewhat lower — 82 ± 8 %. In the HE province, where PP is higher, relative nutrients consumption is somewhat higher, too, at 56 ± 5, 77 ± 4, 88 ± 3 for P, N, and Si, respectively; in the SN province the respective values are 44 ± 11, 61 ± 8, and 82 ± 8 %. That is, in this case the following pattern was confirmed: introducing peridinium plankton into the cold Arctic Ocean waters, where algocenosis is comprised of diatoms only, leads to higher PP values.

During the photosynthesis peak, NCP_{Si} : NCP_N ratio in the HE province was the highest among the waters surrounding the Svalbard archipelago, namely 2.9–3.1 (average temperature in the euphotic layer being as low as 0.90 °C), while in the waters located to the north of the archipelago (SN province) this ratio varied within the range of 2.2–2.4 (at an average water temperature of 2.53 °C). These data show that mineral nutrients supply rate in the euphotic layer does not necessarily correlate with the water temperature.

Conclusions

A new approach has been developed and demonstrated to assessing a part of total biological production in marine ecosystems, that is primary production. The approach combines an estimate of relative volumes of basic water masses using salinity and $\delta^{18}O$ stable isotope with a primary production estimate based on the volumes of these water masses and nutrients (P, N, and Si) concentrations therein. The technique allows for a primary production estimate based on the nutrients consumption. By using a combination of $\delta^{18}O$ isotope parameter (with an intention to add δD in the future), salinity, and nutrients composition, the present methodology allows to consider the domain of the marine ecosystem that comprises its hydrological, hydrochemical, and hydrobiological (phytoplankton) processes as a single system of their interrelations.

Within this methodology, the primary production values themselves are an ultimate result of evaluating and analysing a set of intermediate parameters, each parameter belonging either to the hydrology, hydrochemistry, or hydrobiology block.

The hydrology block covers water composition in terms of basic water masses, that is, Atlantic, river, and ice waters. Hydrochemistry block concerns measured nutrient reserves, conservative reserve, nutrient inflow/outflow in the euphotic layer, nutrient remineralization coefficient. Using these parameters allows to obtain true stoichiometric ratios of C : Si : N : P for each sample examined. It also allows to calculate relative reserve/consumption of the nutrient, similarly to water saturation with dissolved oxygen, which in itself provides for new opportunities for analysing the hydrochemical regime of a marine water area. In the hydrobiology block, relative biomasses (in terms of carbon) of diatoms and peridinium planktons were used as intermediate parameters, to be supplemented later by total relative biomass of the remaining phytoplankton.

The technique was validated in the waters surrounding the Svalbard archipelago. The primary production values obtained were compared to model calculation data published by other authors; not only has this verification shown that the results are consistent, but also that the technique described possesses several advantages. Also, PP values in the Atlantic waters of the West and South Spitsbergen Currents were obtained at a period when photosynthesis rate was the highest; these PP values were 90 ± 8 and 131 ± 9 gCm^{-2}. In these waters, the remaining nutrients reserves do not serve as a limiting factor for photosynthesis development.

In the cold waters incoming from the Arctic Ocean, primary production values were several times lower, namely 19.0 ± 1.4 gCm^{-2}. It was also shown that in these waters diatoms comprised nearly 100 % of the algocenosis, and silicon was a limiting factor of photosynthesis. This is a unique situation that allows to obtain a "pure" C : Si : N : P ratio. While according to Sverdrup this ratio (in terms of mass) in diatoms was 100 : 93 : 18.2 : 2.7, the data obtained led to a ratio of 100 : 109.7 : 18.9 : 2.7. The ratios are rather close to each other. Nevertheless, calculated silicon consumption is still somewhat higher than that in the Table, namely 1.17 times higher.

ECOLOGY

References

Arzhanova, N. V., Zubarevich, V. L., and Sapozhnikov, V. V. 1995a. Seasonal changes of the nutrients stocks in the euphotic layer and assessment of primary production in the Bering Sea; pp. 162–179 in Complex studies of the ecosystem of the Bering Sea. Collection of scientific works. Russian Federal Research Institute of Fisheries and Oceanography Press. Moscow. (In Russian)

Arzhanova, N. V. and Zubarevich, V. L. 1995b. Chemical composition of the bioproductivity of the Sea of Okhotsk; pp. 84–90 in Complex studies of the ecosystem of the Sea of Okhotsk. Collection of scientific works. Russian Federal Research Institute of Fisheries and Oceanography Press. Moscow. (In Russian)

Arzhanova, N. V. and Zubarevich, V. L. 1997. Seasonal changes in the content of biogenic elements in the Sea of Okhotsk as a basis for assessing phytoplankton production; pp. 84–90 in Complex studies of the ecosystem of the Sea of Okhotsk. Collection of scientific works. Russian Federal Research Institute of Fisheries and Oceanography Press. Moscow. (In Russian)

Batrak, K. V. 2009. Hydrochemical indicators of the structure and bioproductivity of Antarctic waters. PhD in Geographical Sciences thesis abstract. Moscow, 26 pp. (In Russian)

Bauch, D., Schlosser, P., and Fairbanks, R. F. 1995. Freshwater balance and the sources of deep and bottom waters in the Arctic Ocean inferred from the distribution of $H_2{}^{18}O$. *Progress in Oceanography* 35:53–80. https://doi.org/10.1016/0079-6611(95)00005-2

Bauch, D., Erlenkeuser, H., Stanovoy, V., Simstich, J., and Spielhagen, R. F. 2003. Freshwater distribution and brine waters in the southern Kara Sea in summer 1999 as depicted by $d^{18}O$ results; pp. 73–90 in R. Stein, K. Fahl, D. K. Fuetterer, E. Galimov (eds), Proceedings in Marine Science, Siberian River Run-off in the Kara Sea: Characterization, quantification, variability and environmental significance. Vol. 6. Elsevier. Amsterdam.

Bauch, D., Erlenkeuser, H., and Andersen, N. 2005. Water mass processes on Arctic shelves as revealed from $\delta^{18}O$ of H_2O. *Global and Planetary Change* 48:165–174. http://doi.org/10.1016/j.gloplacha.2004.12.011

Bauch, D., Dmitrenko, I., Wegner, C., Holemann, J., Kirillov, S., Timokhov, L., and Kassens, H. 2009. Exchange of Laptev Sea and Arctic Ocean halocline waters in response to atmospheric forcing. *Journal of Geophysical Research: Oceans* 114:C005008. https://doi.org/10.1029/2008JC005062

Bauch, D., Groger, M., Dmitrenko, I., Holemann, J., Kirillov, S., Mackensen, A., Taldenkova, E., and Andersen, N. 2011. Atmospheric controlled freshwater release at the Laptev Sea continental margin. *Polar Research* 30:5858. https://doi.org/10.3402/polar.v30i0.5858

Bauch, D., Torres-Valdes, S., Polyakov, I., Novikhin, A., Dmitrenko, I., McKay, J., and Mix, A. 2014. Halocline water modification and along-slope advection at the Laptev Sea continental margin. *Ocean Science* 10(1):141–154. https://doi.org/10.5194/os-10-141-2014

Bauch, D., Cherniavskaya, E., and Timokhov, L. 2016. Shelf basin exchange along the Siberian continental margin: Modification of Atlantic Water and Lower Halocline Water. *Deep Sea Research Part I: Oceanographic Research Papers* 115:188–198. https://doi.org/10.1016/j.dsr.2016.06.008

Bauch, D. and Cherniavskaia, E. 2018. Water mass classification on a highly variable arctic shelf region: Origin of Laptev sea water masses and implications for the nutrient budget. *Journal of Geophysical Research: Oceans* 123:1896–1906. https://doi.org/10.1002/2017JC013524

Bordovsky, O. K. and Ivanenkov, V. N. 1979. Oceanology. Ocean Chemistry. Vol. 1. 518 pp. Nauka Publ. Moscow. (In Russian)

Boyer, T. P., Garcia, H. E., Baranova, O. K., Locarnini, R. A., Mishonov, A. V., Grodsky, A., Paver, C. R., Weathers, K. W., Smolyar, I. V., Reagan, J. R., Seidov, D., and Zweng, M. M. 2019. World Ocean Atlas 2018: Product Documentation. https://www.ncei.noaa.gov/products/world-ocean-atlas

Boyer, T. P., Baranova, O. K., Coleman, C., Garcia, H. E., Grodsky, A., Locarnini, R. A., Mishonov, A. V., Paver, C. R., Reagan, J. R., Seidov, D., Smolyar, I. V., Weathers, K., and Zweng, M. M. 2018. World Ocean Database 2018. NOAA Atlas NESDIS 87.

Codispoti, L. A., Kelly, V., Thessen, A., Matrai, P., Suttles, S., Hill, V., Steel, M., and Light, D. 2013. Synthesis of primary production in the Arctic Ocean: III. Nitrate and phosphate-based estimates of net community production. *Progress in Oceanography* 110:126–150. https://doi.org/10.1016/j.pocean.2012.11.006

Cooper, L. H. N. 1937. On the ratio of nitrogen to phosphorus in the sea. *Journal of the Marine Biological Association of the United Kingdom* 22:177–182. https://doi.org/10.1017/S0025315400011930

Cooper, L. H. N. 1938. Salt error in determinations of phosphate in sea water. *Journal of the Marine Biological Association of the United Kingdom* 23:171–178. https://doi.org/10.1017/S0025315400054035

Dubinina, E. O., Miroshnikov, A. Yu., Kossova, S. A., and Shchuka, S. A. 2019. Modification of Laptev Sea freshened shelf waters based on isotope and salinity relations. *Geokhimiia* 64(1):3–19. https://doi.org/10.31857/S0016-752564113-19 (In Russian)

Dubinina, E. O., Kossova, S. A., Miroshnikov, A. Yu, and Fyaizullina, R. V. 2017. Isotope (δD, $\delta^{18}O$) composition and the freshwater input to the Kara Sea. *Okeanologiia* 1(57):38–48. (In Russian)

Dugdale, R. C. and Goering, J. J. 1967. Uptake of new and regenerated forms of nitrogen in primary productivity. *Limnology and Oceanography* 12(2):196–206. https://doi.org/10.4319/lo.1967.12.2.0196

Dybwad, C., Assmy, P., Olsen, L. M., Peeken, I., Nikolopoulos, A., Krumpen, T., Randelhoff, A., Tatarek, A., Wiktor, J., M., and Reigstad, M. 2021. Carbon export in the seasonal sea ice zone North of Svalbard from winter to late summer. *Frontiers in Marine Science* 7:525800. https://doi.org/10.3389/fmars.2020.525800

Hill, V., Patricia, J., Matrai, A., Olson, E., Suttles, S., Steele, M., Codispoti, L. A., and Zimmerman, R. C. 2013. Synthesis of integrated primary production in the Arctic Ocean: II. In situ and remotely sensed estimates. *Progress in Oceanography* 110(2013):107–125. https://doi.org/10.1016/j.pocean.2012.11.005

Kivva, K. K. 2014. Assessment of primary production of the Bering Sea using a new approach. *Proceedings of VNIRO* 152:73–84. (In Russian)

Makarevich, P. R. and Oleinik, A. A. 2017. Phytoplankton of the Barents Sea in the spring period: composition and structure in the area of the ice edge. *Proceedings of the Kola Scientific Center. Oceanology* 4:50–58. (In Russian)

Matishov, G. G., Berdnikov, S. V., Zhichkin, A. P., Dzhenyuk, S. L., Smolyar, I. V., Kulygin, V. V., Yaitskaya, N. A., Povazhniy, V. V., Sheverdyaev, I. V., Kumpan, S. V., Tret'yakova, I. A., Tsygankova, A. E., D'yakov, N. N., Fomin, V. V., Klochkov, D. N., Shatohin, B. M., Plotnikov, V. V., Vakul'skaya, N. M., Luchin, V. A., and Kruts, A. A. 2014. Atlas of climatic changes in nine large marine ecosystems of the Northern Hemisphere (1827–2013). NOAA Atlas NESDIS 78, 131 p. https://doi.org/10.7289/V5Q52MK5

Melling, H. and Moor, R. M. 1995. Modification of halocline source waters during freezing on the Beaufort Sea shelf: evidence from oxygen isotopes and dissolved nutrients. *Continental Shelf Research* 15(1):89–113. https://doi.org/10.1016/0278-4343(94)P1814-R

Moiseev, D. V., Zaporozhtsev, I. F., Maximovskaya, T. M., and Dukhno, G. N. 2019. Identification of frontal zones posi-

tion on the surface of the Barents Sea according to in situ and remote sensing data (2008–2018). *Arctic: Ecology and Economy* 2(34):48–63. https://doi.org/10.25283/2223-4594-2019-2-48-63 (In Russian)

Nesvetova, G. I. 2003. Hydrochemical conditions of functioning of the ecosystem of the Barents Sea. Dr. Sci. in Geographical Sciences thesis. Murmansk, 424 pp.

Namyatov, A. A. and Semeryuk, I. A. 2019. Using $\delta^{18}O$ as a tracer of the formation of water masses in the Laptev Sea. Part 2. Quantification of the volume of Atlantic, river and melt water as well as water withdrawn for ice formation. *Russian Meteorology and Hydrology* 44(7):54–63. https://doi.org/10.3103/S1068373919070057

Namyatov, A. A. 2021. $\delta^{18}O$ as a tracer of the main regularities of water mass mixing and transformation in the Barents, Kara and Laptev seas. *Journal of Hydrology* 593:125813. https://doi.org/10.1016/j.jhydrol.2020.125813

Sapozhnikov, V. V. and Metrevely, M. P. 2015. Organic matter stoichiometry as a basis for quantitative studies of production and destruction processes in the ocean; pp. 139–145 in Proceedings of VNIRO. Russian Federal Research Institute of Fisheries and Oceanography Press. Moscow. (In Russian)

Titov, O. V. 2003. Long-term changes in the hydrochemical regime and ecosystem of the Barents Sea. Dr. Sci. in Geographical Sciences thesis. Murmansk, 329 p. (In Russian)

Ostlund, H. G. and Hut, G. 1984. Arctic Ocean water mass balance from isotope data. *Journal of Geophysical Research: Oceans* 89:6373–6381. https://doi.org/10.1029/JC089iC04p06373

Pautova, L. A., Silkin, V. A., Kravchishina, M. D., Yakubenko, V. G., and Chultsova, A. L. 2019. Summer phytoplankton of the northern Barents Sea (75–80° N). *Hydrosphere Ecology* 2(4):8–19. https://doi.org/10.33624/2587-9367-2019-2(4)-8-19 (In Russian)

Redfield, A. C. 1934. On the properties of organic derivatives in sea water and their relation to the composition of plankton; pp. 177–192 in J. Johnstone, James Johnstone Memorial Volume. University Press of Liverpool. Liverpool.

Redfield, A. C. 1958. The biological control of chemical factors in the environment. *American Scientist* 46:205–221.

Reigstad, M., Carroll, J., Slagstad, D., Ellingsen, I., and Wassmann, P. 2011. Intra-regional comparison of productivity, carbon flux and ecosystem composition within the northern Barents Sea. *Progress in Oceanography* 90(1–4):33–46. https://doi.org/10.1016/j.pocean.2011.02.005

Richards, F. A. 1958. Dissolved silicate and related properties of some Western North Atlantic and Caribbean Waters. *Journal of Marine Research* 17:449–465.

Sakshaug, E. 2004. Primary and secondary production in the Arctic Seas; pp. 57–81 in R. Stein, R. W. Macdonald (eds), The organic carbon cycle in the Arctic Ocean. Springer-Verlag. Berlin; Heidelberg. https://doi.org/10.1007/978-3-642-18912-8_3

Sanz-Martín, M., Vernet, M., Cape, M. R., Mesa, E., Delgado-Huertas, A., Reigstad, M., Wassmann, P., and Duarte, C. M. 2019. Relationship between carbonand oxygen-based primary productivity in the Arctic Ocean, Svalbard Archipelago. *Frontiers in Marine Science* 6:468. https://doi.org/10.3389/fmars.2019.00468

Semeryuk, I. A. and Namyatov, A. A. 2018. Using $\delta^{18}O$ as a tracer of the formation of water masses in the Laptev Sea. Part 1. Quantification of ice formation and melting. *Russian Meteorology and Hydrology* 43(9):49–60. https://doi.org/10.3103/S1068373918090054

Slagstad, D., Wassmann, P. F. J., and Ellingsen, I. 2015. Physical constrains and productivity in the future Arctic Ocean. *Frontiers in Marine Science* 2:85. https://doi.org/10.3389/fmars.2015.00085

Sverdrup, H. U., Johnson, M. W., and Fleming, R. H. 1942. The oceans, their physics, chemistry and general biology. 1087 pp. Prentice Hall Inc. New York.

Schmidt, G. A., Bigg G. R., and Rohling, E. J. 1999. Global Seawater Oxygen-18 Database. https://data.giss.nasa.gov/o18data

Schlitzer, R. 2021. Ocean Data View. https://odv.awi.de

Tamelander, T., Reigstad, M., Olli, K., Slagstad, D., and Wassmann, P. 2013. New production regulates export stoichiometry in the ocean. *PLoS ONE* 8(1):e54027. https://doi.org/10.1371/journal.pone.0054027

Terziev, F. S. 1991. Hydrometeorology and hydrochemistry of the seas. Project Sea of the USSR. Vol. 1. Iss. 1. Barents Sea. 280 pp., Gidrometizdat Publ. St. Petersburg. (In Russian)

Vernet, M., Ellingsen, I., Marchese, C., Bélanger, S., Cape, M., Slagstad, D., and Matrai, P. A. 2021. Spatial variability in rates of net primary production (NPP) and onset of the spring bloom in Greenland shelf waters. *Progress in Oceanography* 198:102655. https://doi.org/10.1016/j.pocean.2021.102655

Ward, J. H. 1963. Hierarchical grouping to optimize an objective function. *Journal of the American Statistical Association* 58:236–244. https://doi.org/10.1080/01621459.1963.10500845

Vinogradov, A. P. 1939. The chemical composition of plankton; pp. 189–213 in Proceedings of the Biogeochemical Laboratory, Academy of Sciences of the USSR. Moscow. (In Russian)

Yearbook. Surface water quality of the Russian Federation. Hydrochemical Institute. https://gidrohim.com/node/44 (In Russian)

Appendix

Fractionation of $\delta^{18}O$ and δD during freezing of seawater under natural conditions.
Data were acquired in the Barents Sea in the research vessel "Dalnie Zelency" in March 2021.

Stations	Water salinity, psu	Water (‰)	Ice (‰)	Fractionation (‰)
		$\delta^{18}O$	$\delta^{18}O$	Change in $\delta^{18}O$
47	34.077	0.087	1.790	1.703
43	34.199	–0.059	1.410	1.469
51	34.711	0.066	2.460	2.394
61	34.659	0.072	2.000	1.928
39	33.874	–0.220	1.650	1.870
57	34.691	–0.050	1.440	1.490
		Average value		1.809
		Standard deviation		0.343